EnvironmentAsia
The international journal by the Thai Society of Higher Education Institutes on Environment

EnvironmentAsia 19(2) 2026 16-33
DOI 10.14456/ea.2026.22
ISSN 1906-1714; ONLINE ISSN: 2586-8861

Comparative Adsorption of Fuchsin Acid and Eosin Blue Using Zinc Oxide and Titanium Dioxide Modified Activated Carbon Derived from Plastic Waste

Ayat S. Al-Maliki[1], Dunya A. Al-Abbawy[1*], and Zuhair A. Abdulnabi[2]

[1]*Department of Ecology, College of Science, University of Basrah, Iraq*
[2]*Department of Marine Chemistry, marine sciences center, University of Basra, Iraq*

*Corresponding author: dunya.hussain@uobasrah.edu.iq
Received: January 13, 2026; Revised: February 26, 2026; Accepted: April 7, 2026

Abstract

Activated carbon was synthesized from plastic waste (polyethylene terephthalate) and oxidized to improve its surface properties. Zinc oxide (ZnO) nanoparticles were produced via co-precipitation, and titanium oxide nanoparticles (TiO_2) were synthesized using mechanical milling. The prepared materials were characterized using Fourier-transform infrared (FTIR), X-ray diffraction (XRD), scanning electron microscopy (SEM), and EDX analyses. The nanostructured oxides were subsequently loaded onto the activated carbon surface, and the resulting composites were further analyzed using FTIR, XRD, SEM, EDX, BET surface area, and zeta potential measurements. The obtained adsorbent was applied to remove two dyes (Eosin Blue and Fuchsin Acid) from an aqueous solution under varying conditions, including contact time, pH, temperature, and agitation speed. The removal efficiencies reached 72.49% for Eosin Blue and 89.05% for Fuchsin Acid. Adsorption isotherm studies indicated that the adsorption of Eosin Blue followed the Langmuir model with a maximum adsorption capacity of 164.64 mg/g, whereas Fuchsin Acid was better described by the Freundlich model, with a higher capacity of 519.87 mg/g. Furthermore, the thermodynamic parameters confirmed the feasibility, spontaneity, and mixed endothermic-exothermic behavior of the adsorption process.

Keywords: Dyes; Nanoparticles; Removal efficiency; Titanium dioxide

1. Introduction

The rapid expansion of industrial activities has intensified global environmental challenges, particularly the deterioration of water quality. Water is vital for sustaining all forms of life (Khan *et al.,* 2017), and its contamination with chemical pollutants has become a major concern for researchers and regulatory bodies (Crini and Lichtfous, 2019). Various hazardous organic pollutants, including dyes, hydrocarbons, pesticides, and pharmaceuticals, have been detected in different environmental compartments such as water, soil, and air (Crini & Lichtfouse, 2019; Tripathi *et al.,* 2023). Regional studies in Basra have also reported the accumulation of polycyclic aromatic hydrocarbons on biological collectors such as spider webs, highlighting the extent of anthropogenic pollution in the area (Taher *et al.,* 2023). They originate from various industries, including textiles, food processing, plastic, rubber, paper, leather, cosmetics, and ink manufacturing (Nayeri and Mousavi, 2020). Industrial wastewater typically contains dye concentrations of 100-5000 mg/L, with 15-20% of synthetic dyes discharged directly

into water bodies, while about 10% resist degradation under natural conditions (Alvez-Tovar *et al.,* 2025).

Dyes are classified according to ionic charge into anionic dyes, cationic dyes, and neutral dyes (Bellot-Gurlet *et al.,* 2023). Fuchsin Acid (FA), an acidic triamine dye, has the formula $C_{20}H_{17}N_3Na_2O_9S_3$ (Abou-El-Souod and El-Sheekh, 2016). Eosin Blue (EB), another acidic dye belonging to the xanthine class, has the molecular formula $C_{20}H_8Br_4Na_2O_5$. It is extensively applied in pharmaceuticals, cosmetics, inks, paints, and cytoplasmic staining for disease diagnostics (Rahman, 2017; Tripathi *et al.,* 2023).

Wastewater containing dyes and heavy metals necessitates effective treatment strategies (Crini and Lichtfous, 2019; Tolkou and Kyzas, 2024). Advanced methods, including adsorption, membrane filtration and oxidation are increasingly applied, with adsorption standing out due to its simplicity, cost-effectiveness, and high pollutant removal efficiency (Aremu *et al.,* 2021; Mehta *et al.,* 2024). Recent studies highlight the superior reactivity and reusability of nanostructures and polymer-based adsorbents (Rezania *et al.,* 2022). For example, Al-Mosawi *et al.* (2022) demonstrated the strong chelating ability of polyurethane-supported Schiff base resins for metal removal, while Jumaa *et al.* (2024) showed the enhanced performance of TiO_2 anoplasties in treating Basra River water.

Conventional adsorbents such as activated carbon (AC) and metal nano oxides remain widely applied for removing organic and inorganic pollutants (Bhatnager *et al.,* 2013; Paul *et al.,* 2020). Additionally, low-cost adsorbents derived from agricultural wastes and recycled materials have shown promising dye removal performance (Masoudian *et al.,* 2019; Muttil *et al.,* 2023). Recently, the efficiency of activated carbon has been further enhanced by incorporating metal oxide nanoparticles, including Fe_2O_3, ZnO, Al_2O_3, and TiO_2, to improve surface area, reactivity, and porosity (Nguyen *et al.,* 2020), supported by their nontoxicity, stability, affordability, and high efficiency (Wang *et al.,* 2021; Tolkou and Kyzas, 2024).

This study investigates the removal of Fuchsin Acid and Eosin Blue dyes from aqueous solutions using activated carbon derived from plastic waste (polyethylene terephthalate) and modified with TiO_2 and ZnO nanoparticles to enhance adsorption performance. Adsorption experiments were conducted using synthetic dye-contaminated wastewater prepared under controlled laboratory conditions to evaluate the efficiency of the developed nanocomposite adsorbent.

2. Methodology

2.1 chemicals

All chemical materials were of analytical grade and used as received. Several analytical-grade chemicals were used in the present study, including Eosin Blue and Fuchsin Acid (BDH, UK). Ammonium hydroxide (25%), sodium hydroxide, potassium hydroxide, and titanium dioxide were purchased from Merck (Germany). Ethanol (96%) was used as the solvent and supplied by Fisher Chemical Company. Hydrochloric acid (37%) and nitric acid (65%) were obtained from GCC Company, and sulfuric acid (95%) was purchased from J. T. Baker Company. Finally, zinc acetate dihydrate Zn $(CH_3COO)_2.2H_2O$ was obtained from Riedel-De Haen Agseelze-Hannover.

2.2 Instrumentation

The elemental content and morphology were characterized using EDS and SEM analyses, respectively, using a Vega A3 TESCAN microscope at 20 kV. XRD was used to identify the crystalline phases of the prepared compounds at a wavelength of 1.54 Å, using Kα-Copper as the source model from the Philips company (PW1730). The maximum wavelength was determined using a UV-Vis spectrophotometer (model UV-1800, Shimadzu, Japan).

2.3 Preparation of activated carbon

Plastic waste samples, primarily polyethylene terephthalate (PET) from collected plastic bottles, followed the method reported in previous studies (Yulismanen *et al.,* 2017; Ayyalusamy and Mishra, 2018).

The samples were washed several times with distilled water, dried at 65 °C for 4 hours, cut into small pieces, ground, and sieved to 2 mm. The obtained fine material was washed again and dried at 65 ºC for 8 hours.

A total of 25 g of the sieved plastic waste was soaked in 25 mL of sulfuric acid for 2 hours, then heated on a hot plate at 90 °C for an additional 2 hours until the material gradually turned black. The samples were left to cool for 15 min, washed repeatedly with distilled water, and dried at 80 °C for 4 hours. Carbonization was then carried out in a furnace at 300 °C for 3 hours, followed by washing and filtration to obtain the solid black product, which was finally dried at 80 °C for 5 hours.

Functionalization of activated carbon was performed based on Abdulnabi *et al.* (2021). A 20 g portion of the carbonized product was mixed with 300 mL of 10% HCl and stirred overnight at room temperature for purification. Afterwards, filtration and drying at 80 °C for 6 hours, 10 g of the purified activated carbon was oxidized using 32.5% Nitric acid at 60 °C. The mixture was stirred continuously for 6 hrs. The material was washed with deionized water until neutrality was reached and then dried at 80 °C For 10 hrs.

2.4 Preparation of nano oxides

2.4.1 Titanium dioxide

A 25 g sample was mechanically size-reduced with TiO_2 powder in a locally fabricated ball mill to achieve particle size reduction and enhanced surface area. The resulting powder was washed several times with ethanol to remove residual impurities, followed by drying in an oven at 80 °C for 240 min, yielding a high product recovery.

2.4.2 Zinc oxide

Zinc oxide was prepared according to the method described by Seow *et al.* (2008) and Raheem *et al.* (2025) by dissolving 2.19809 g of zinc acetate dihydrate in 300 mL of distilled water. Then, the potassium hydroxide solution was prepared by dissolving 1.2155 g in 50 mL of distilled water and adding it to the zinc acetate solution, where the formation of a white precipitate was observed. The pH of the solution was adjusted using a dilute solution of 1% HCl and NaOH. Consequently, the solution was filtered and dried at 100 °C in an oven for 120 min. Finally, the white precipitate was calcined in a furnace at 400 °C for 180 min.

TiO_2 and ZnO nanoparticles were loaded onto synthetic activated carbon by mixing 0.04 g of each nano-oxide with 0.2 g of activated carbon in distilled water under ultrasonication, followed by the hydrothermal method in a stainless-steel autoclave at 180 °C for 6 hours. In the final step, a new solid compound was obtained by separating and drying it at 80 °C for 3 hours.

2.4.3 Preparation of standard solutions of the dyes

To determine the maximum adsorption wavelength of each dye (Eosin Blue and Fuchsin Acid), a stock solution of 1000 mg/L was initially prepared, and then 20 mg/L was prepared from it and measured using a UV-Vis spectrophotometer within a scanning range of 200–800 nm. The results indicated maximum adsorption wavelengths of 518.5 nm for Eosin Blue and 546.5 nm for Fuchsin Acid.

2.4.4 Adsorption experiments

The study aims to remove two dyes from their aqueous solution, which belong to different dye classes: the xanthine class for Eosin Blue and the triamine class for Fuchsin Acid (Abou-El-Souod and El-Sheekh, 2016; Rahman, 2017) (Figure 1).

Adsorption experiments were conducted to evaluate the removal efficiency of the Eosin Blue and Fuchsin Acid dyes from aqueous solutions using the prepared adsorbent. The experiments were performed separately for each dye under batch adsorption conditions at room temperature. Four operational parameters were investigated to determine the optimum adsorption conditions: contact time, pH, temperature, and shaking speed.

For equilibrium analysis, the adsorption data were evaluated using the Langmuir and Freundlich isotherm models, respectively.

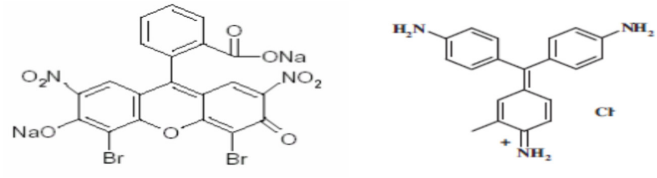

Eosin Blue (EB) Fuchsin Acid

Figure 1. Chemical structures of the studied dyes, used in the adsorption experiments

Both models were applied to the experimental results, and the most suitable model was selected based on the correlation coefficient (R^2) and consistency of the calculated parameters with the theoretical assumptions of each model.

The adsorption data for Eosin Blue showed a better fit to the Langmuir model, indicating monolayer adsorption on a relatively homogeneous surface. In contrast, the adsorption of Fuchsin Acid was better described by the Freundlich model, suggesting multilayer adsorption on a heterogeneous surface.

Thus, the most appropriate isotherm model for each dye was determined empirically based on the experimental data rather than predetermined. The R^2 values and isotherm parameters have been included in the manuscript text and figures within the Isotherm Study subsection to enhance transparency.

Initial dye concentrations of 100 mg/L for Eosin Blue and 200 mg/L for Fuchsin Acid were used in synthetic aqueous solutions as representative values within the typical range for industrial dye effluents (100-5000 mg/L, Alvez-Tovar *et al.,* 2025). For each experiment, 10 mL of the dye solution was placed in a 50 mL tightly sealed conical flask, and 10 mg of the prepared adsorbent was added. The mixtures were agitated at a constant shaking speed of 150 rpm at room temperature and neutral pH for varying contact times to determine the equilibrium adsorption time for each dye. All adsorption experiments were conducted individually for each dye system to avoid competitive adsorption. The adsorption experiments were performed in triplicate, and the reported values represent the average of three independent measurements.

After adsorption, the adsorbent surface was isolated by centrifugation to obtain the residual concentration of each dye in the filtered solution by measuring the maximum wavelength (518.5 and 546.5 nm for Eosin Blue and Fuchsin Acid, respectively). The adsorption percentage and adsorption capacity were computed using the following equations (Krishnan *et al.,* 2020).

$$\% AD = [(C_o - C_e)/C_o] \times 100 \quad (1)$$

$$Q_e\ (mg/g) = [V \times (C_o - C_e)] / W \quad (2)$$

where the %AD represents the percentage of the adsorption process, C_o and C_e are the initial and equilibrium concentrations of each dye's solutions, Q_e is the adsorption capacity by unit mg/g, V is the volume of solution used (L), and W is the amount of adsorbent by unit gram.

2.4.5 Isotherm study

The isotherm study can help us understand the adsorption mechanism between the dye molecules (Salleh *et al.,* 2011). The relationship between adsorbate molecules and the adsorbent surface can be described according to the Gils classification. Equilibrium adsorption data obtained from the experiments were analyzed using widely applied isotherm models to determine the most appropriate description of the adsorption behavior. In this study, two isotherm models were selected: Langmuir and Freundlich. The adsorption capacity was calculated using the Langmuir equation (Nageeb, 2013) by plotting a graph between C_e and Q_e. The Langmuir equation is expressed as follows:

$$C_e/Q_e = (1/ (Q_{max} \times K_L)) + (C_e/Q_{max}) \quad (3)$$

where Q_{max} is the adsorption capacity for adsorbing dye molecules from their aqueous solutions under changing concentration at a fixed temperature, and K_L is the Langmuir constant in unit L/mg.

The Freundlich equation can be summarized as follows:

$$\text{Log } Q_e = \text{Log } K_f + (\text{Log } C_e/n) \quad (4)$$

In this context, Kf represents the Freundlich constant, which indicates the adsorption capacity and is measured in units of L/g, while n denotes the heterogeneity factor, which reflects the intensity of adsorption. The value of the heterogeneity factor indicates the preferred selection of the adsorption process, where if the n value is equal to zero (n=0), it indicates that the adsorption reaction is irreversible, while if the value of n is lower than one and bigger than zero (0<n<1), the adsorption process can be called unfavorable. Finally, if the n value is bigger than one (n>1), this adsorption process is called favorable (Bahramifar *et al.,* 2015).

3. Results and Discussion

3.1 Characterization of the prepared compound

3.1.1 Fourier transform infrared spectroscopy (FTIR)

FTIR analysis was employed to identify the functional groups of the synthesized materials and to verify their structural modifications. The spectrum of activated carbon derived from plastic waste showed aromatic C-H stretching at 3063.7 cm^{-1} and aliphatic C-H stretching at 2970.6 and 2814.6 cm^{-1} (Remmani *et al.,* 2021). A strong absorption near 1677 cm^{-1} was attributed to C=C and C=O vibration (Liu *et al.,* 2018). Additional bands at 1572.4-1418 cm^{-1} confirmed the presence of benzene rings, while those at 1282.7 and 1014.7-1110.2 cm^{-1} were assigned to C-O and C-O-C groups.

After oxidation with nitric acid, a broad band at 3400 cm^{-1} appeared, which confirms the successful presence of hydroxyl groups.

The formation of zinc oxide was confirmed by peaks at 498.14 and 624.7 cm^{-1}, while TiO_2 was 1057.3 and 447.09 cm^{-1} (Djamel *et al.,* 2023). Upon loading activated carbon with ZnO and TiO_2, characteristic peaks of these oxides appeared alongside reduced intensities of carbon functional groups, indicating the successful deposition of ZnO and TiO_2 on the carbon surface in Figures 2-3.

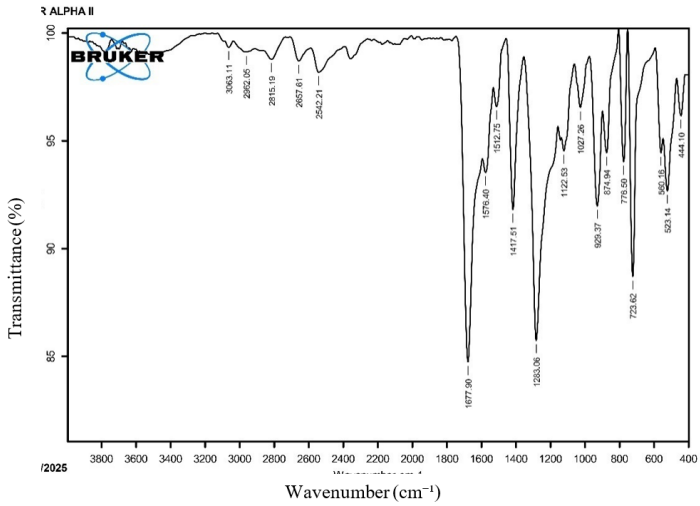

Figure 2. Fourier-transform infrared (FTIR) spectrum of activated carbon (AC) synthesized from plastic waste; showing the characteristic surface functional groups responsible for adsorption

3.1.2 BET analysis

The porous structures of adsorbents strongly influence their performance. The surface area was determined using the BET and BJH methods based on nitrogen adsorption-desorption at 77 K. Results indicated that carbon composites loaded with Zn-Ti oxides achieved a higher surface area (9.577 m^2/g), indicating improved adsorption efficiency (Table 1).

Activated carbon is well known for its well-developed porous structure and high surface area, which are critical parameters for adsorption. The surface area and pore structure of the AC materials were found to be within the range of 500–1500 m^2/g, pore diameters between 1–5 nm, and pore volumes between 0.3 and 1.2 cm^3/g, depending on the raw material used (Bhatnagar *et al.,* 2013; Afroze and Sen, 2018; Nayeri and Mousavi, 2020). These surface features are responsible for providing active sites for adsorption and facilitating the transportation of target pollutant molecules to the active sites within the material structure. Hence, activated carbon and its various modified forms are among the most used adsorbents for removing organic dyes and other impurities from wastewater.

The surface area is a critical parameter that affects the adsorption capacity of an adsorbent material. The surface area of the material was determined using BET and BJH techniques from the nitrogen adsorption-desorption isotherms plotted at 77 K. The surface area of the synthesized AC–ZnO–TiO_2 composite material is found to be 9.577 m^2/g, as shown in Table 1.

3.1.3 X-ray powder diffraction

X-ray diffraction was employed to determine the crystalline phase, crystallite size, and structural features of the prepared materials. Distinct diffraction peaks were observed at $2\theta = 21.3^o$, 23.05^o, 24.86^o, 25.59^o,

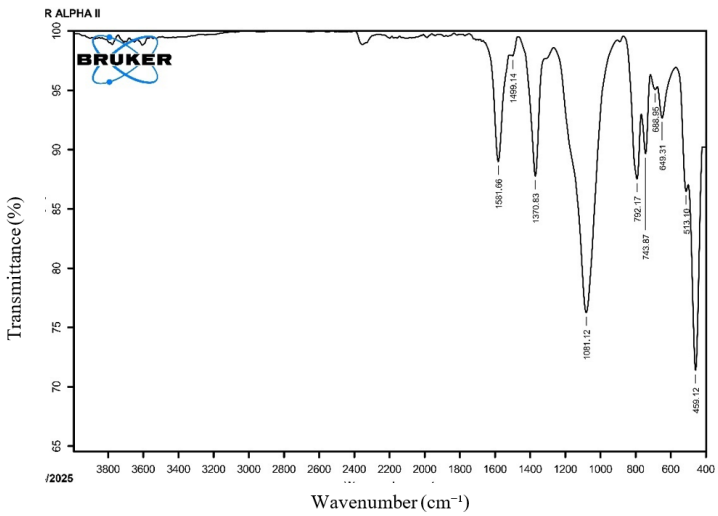

Figure 3. FTIR spectrum of the AC–ZnO–TiO_2 composite illustrates the characteristic functional groups and confirms the successful incorporation of ZnO and TiO_2 nanoparticles onto the activated carbon surface

Table 1. The textural properties of the synthesized AC–ZnO–TiO_2 composite were determined using BET nitrogen adsorption–desorption analysis

Adsorption surface	Pore type	Surface Area (m^2/g)	Pore volume (cm^3/g)	Pore diameter (nm)
AC-ZnO-TiO_2	Micropores	9.577	0.0322	1.2

23.05º, 24.86º, 23.05º,24.86º,25.59º, 32.08º, and 38.19º, consistent with activated carbon and the standard reference (JCPDS Card no. 41-1487). The characteristic peaks observed at 25.59º confirm the successful synthesis of activated carbon from plastic waste.

The XRD pattern of ZnO exhibited sharp peaks at 2θ = 23.03º, 25.40º, 34.77º, 36.56º, 38.35º, 47.9º, 56.86º, 63.38º, 66.9º, 69.72º, and 77.8º, which match the standard ZnO pattern (JCPDS Card no. 36-1415). The average crystallite size was calculated using the Debye-Scherrer equation and appeared to be 24.4 nm, which confirms the success in preparing nanoparticles of zinc oxide.

TiO_2 synthesized via mechanical milling exhibited diffraction peaks at 2Θ = 26.65º, 36.55º, 39.47º, 42.44º, 45.81º, 48.08º, 50.13º, 55.1º, 59.94º, and 68.24º that are consistent with JCPDS card no. 021-1272. The average crystallite size after calculation was 36.33 nm, confirming the titanium dioxide prepared within nanoparticles by using the milled method.

Activated carbon loaded with ZnO and TiO_2 exhibited characteristic peaks at 2θ = 12.55°, 21.3°, 24.67°, 25.92°, and 26.85° that belong to activated carbon, and also new characteristic peaks were observed at 28.14°, 33.04°, 40.04°, 42.09°, 45.92°, 50.57°, and 60.51°, which belong to the existence of titanium oxide, while ZnO reflection appeared at 31.04°, 35.95°, 37.32°, 38.35°, 48.51°, 57.27°, and 64.77°. The apparent characteristic peak of TiO_2 and ZnO appeared to be successfully loaded onto the activated carbon surface. The crystallite size calculated using the Debye-Scherrer equation was 18.94 nm. All the results of XRD are in Figure 4-5.

3.1.4 Scanning Electron Microscopy (SEM) Analysis

Scanning electron microscopy (SEM) was used to examine the surface appearance and structural characteristics of the synthesized materials. Figure 6 illustrates that the activated carbon derived from plastic waste possesses a notably rough and porous surface, featuring irregular pores and channels. These pores may serve as active sites for adsorption and facilitate the movement of dye molecules within the adsorbent.

The addition of metal oxide nanoparticles resulted in a visibly altered surface morphology of the films. Figure 7 shows a scanning electron microscopy (SEM) image of the AC–ZnO–TiO_2 composite. The image shows ZnO and TiO_2 nanoparticles as small particles spread across the carbon surface. The nanoparticles were efficiently distributed within the

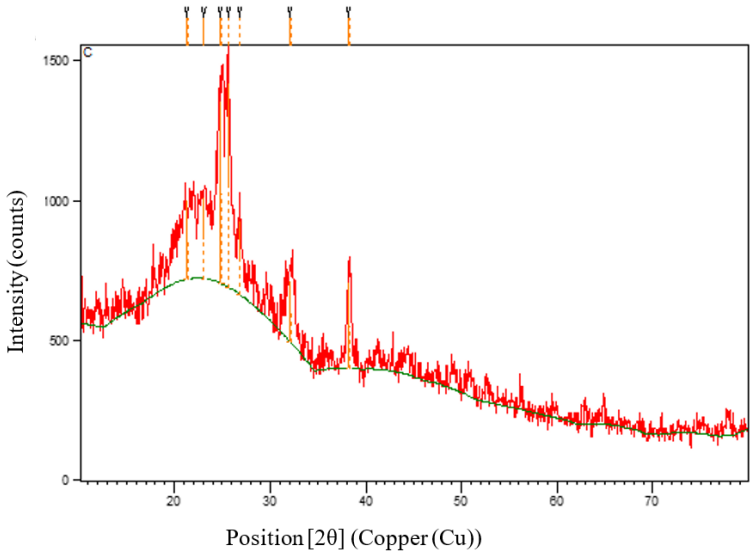

Figure 4. X-ray diffraction (XRD) pattern of the activated carbon (AC) derived from plastic waste indicates the crystalline structure of the prepared carbon material

porous structure of the activated carbon. This renders the surface less homogeneous and provides additional sites for molecular adhesion, enhancing the adsorption capacity of the composite for various molecules. The composite exhibited an average particle size of approximately 24.82 nm, which closely aligns with the crystallite size determined by XRD analysis (≈19.94 nm).

The data confirmed the successful incorporation of ZnO and TiO_2 nanoparticles onto the activated carbon surface, demonstrating that the modification technique produced a nanostructured porous composite with improved surface characteristics, rendering it suitable for adsorption applications (Figures 6–7).

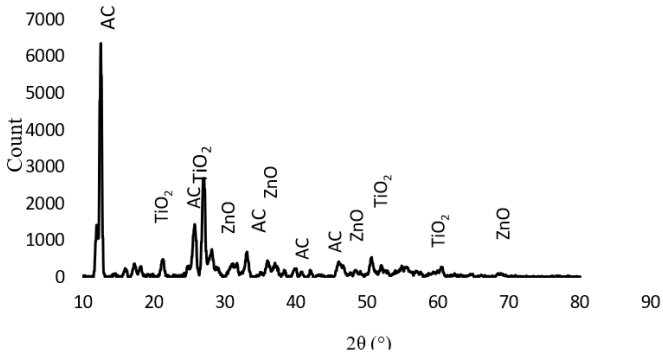

Figure 5. X-ray diffraction (XRD) pattern of the AC–ZnO–TiO_2 composite shows diffraction peaks corresponding to activated carbon and the loaded ZnO and TiO_2 nanoparticles

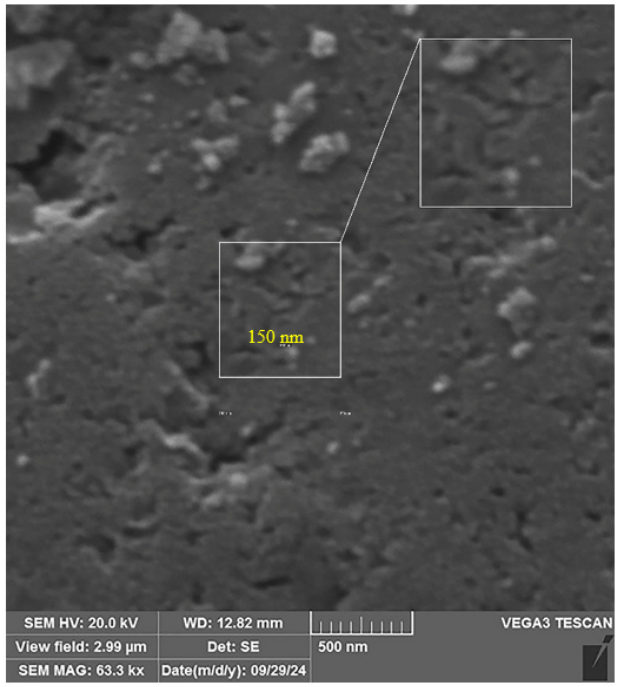

Figure 6. Scanning electron microscopy (SEM) image of activated carbon (AC) derived from plastic waste illustrates the surface morphology and porous structure

3.1.5 Energy Dispersive X-ray (EDX) Analysis

EDX analysis was performed to identify the elemental composition of the prepared nanomaterials and validate their successful synthesis. For ZnO, characteristic peaks of zinc and oxygen were observed, confirming the formation of ZnO nanoparticles, while the presence of a gold peak originated from the coating process.

On the other hand, the clear peaks correspond to titanium and oxygen, which confirm TiO2 and refer to successful preparation through mechanical milling.

The activated carbon derived from plastic waste revealed strong signals of carbon and oxygen that were consistent with the oxidation treatment, which increased the oxygen content and validated the incorporation of oxygen-containing functional groups.

For the composite, activated carbon loaded with ZnO and TiO_2 displayed corresponding peaks of C, O, Zn, and Ti, which are confirming the successful integration of these oxides onto the activated carbon surface. The C/O ratio for the activated carbon composite significantly decreased compared to the C/O ratio of the activated carbon alone, indicating effective functionalization through the loading of metal oxides. All results of EDX are in Figures 8-9.

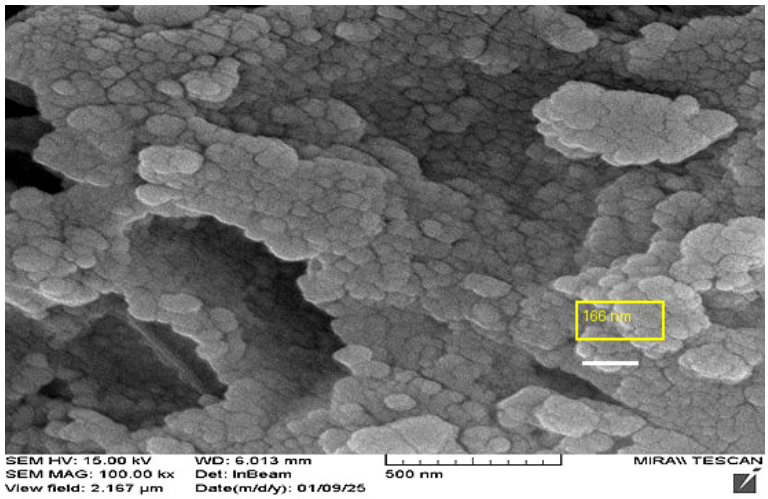

Figure 7. SEM micrograph of the AC–ZnO–TiO_2 composite showing the distribution of ZnO and TiO_2 nanoparticles on the activated carbon surface

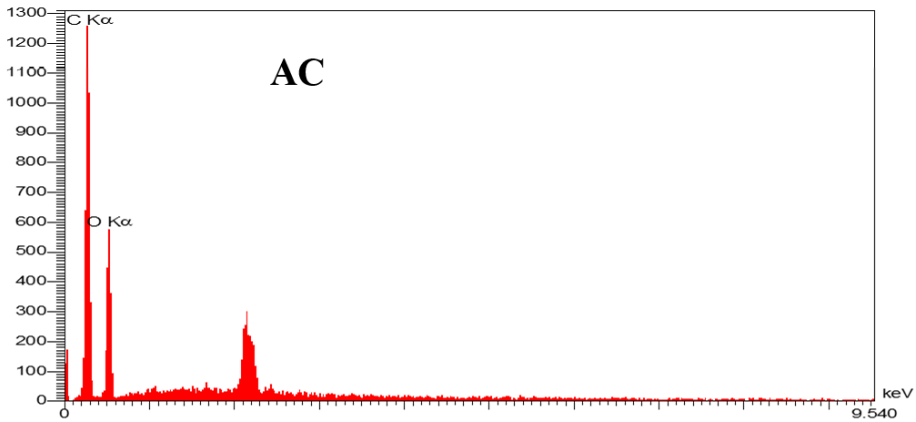

Figure 8. Energy dispersive X-ray (EDX) spectrum of activated carbon (AC) confirms the elemental composition of the prepared carbon material

3.1.6 Zeta potential measurement

Zeta potential analysis offers information about surface charges and colloidal stability, both critical for adsorption performance. The AC-ZnO-TiO2 showed a value of -37.4 mV. The AC-ZnO-TiO_2 exhibited a negative surface charge and high stability (Fernández-Peña *et al.,* 2024) in Figure 10.

3.2 Adsorption Study

Many factors that can negatively or positively affect the adsorption efficiency have been studied as follows;

3.2.1 Effect of Equilibrium Time

The equilibrium time was examined within 5-360 min, under fixed conditions. The results showed that Eosin Blue reached equilibrium at 120 minutes with a removal percentage of 9.81%, while Fuchsin Acid dye reached equilibrium at 240 minutes with a removal percentage of 79.03%. Moreover, the Fuchsin Acid dye was recorded as having a higher adsorption capacity than Eosin Blue (Figures 11-12).

3.2.2 Effect of pH

The pH effect was evaluated within the range of 3 to 9 under fixed experimental conditions. The results indicated that Eosin Blue achieved its highest removal of 47.51% at a low pH value of 3. While Fuchsin Acid recorded the highest removal ratio of 88.90% at pH 8, this confirms the dye's strong affinity for negatively charged surfaces under alkaline conditions.

3.2.3 Effect of Temperature

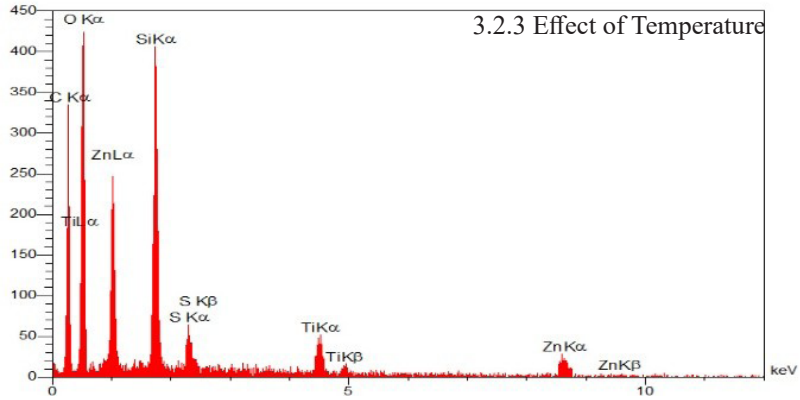

Figure 9. EDX spectrum of the AC–ZnO–TiO_2 composite confirming the presence of carbon, oxygen, zinc, and titanium elements

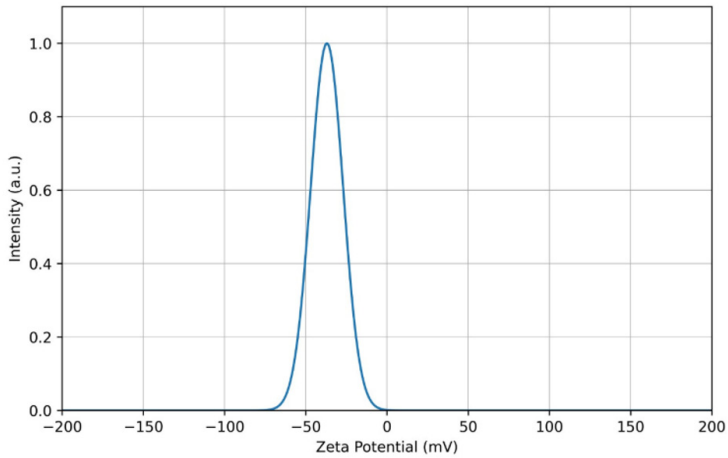

Figure 10. Zeta potential measurement of the AC–ZnO–TiO_2 composite indicating the surface charge and stability of the prepared adsorbent

The temperature study, with a range of 25 ºC to 65 ºC, showed that eosin blue removal increased with temperature, reaching a maximum of 66.03% at 65 ºC. Fuchsin Acid achieved its highest of 88.98% at 25 ºC, indicating temperature-sensitive behavior (Alwi *et al.,* 2020).

3.2.4 Effect of agitation speed

The agitation study showed Eosin Blue achieved its highest removal, 72.49%, at 100 rpm. Furthermore, the removal of Fuchsin A dye increases with decreasing agitation speed at 50 rpm by about 89.05%.

Following the analysis of the four parameters, the ideal circumstances for the elimination of Eosin blue and Fuchsin Acid were established, as detailed in Table 2. The adsorption efficiency (%) of Eosin Blue and Fuchsin Acid was calculated as removal efficiency based on the difference between the initial dye concentration and the equilibrium concentration after adsorption. It was 89.05% for Fuchsin Acid and 72.49% for Eosin Blue.

3.2.5 Adsorption Isotherms

After completing the adsorption process of Eosin Blue and Fuchsin Acid onto modified activated carbon with metal oxide nanoparticles, the adsorption isotherms were examined. According to Raheem *et al.* (2025) The thermodynamic experiment was carried out by preparing different concentrations of

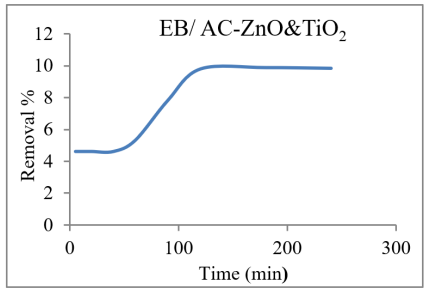

Figure 11. Effect of contact time on the adsorption of Eosin Blue (EB) onto the AC–ZnO–TiO_2 composite

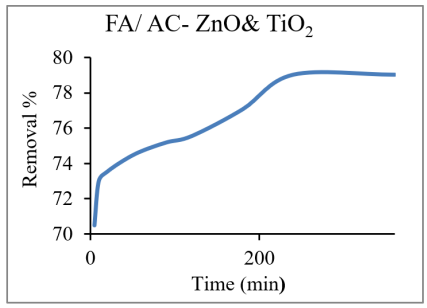

Figure 12. Effect of contact time on the adsorption of Fuchsin Acid (FA) onto the AC–ZnO–TiO_2 composite

Table 2. Optimal experimental conditions for the adsorption of Eosin Blue (EB) and Fuchsin Acid (FA) onto the AC–ZnO–TiO_2 composite, including initial dye concentration (C0), temperature, pH, equilibrium time, agitation speed, and removal efficiency

Dye	C_0 (mg/L)	Temperature (ºC)	pH	Equilibrium time (min)	Agitation Speed (rpm)	Removal Efficiency (%)
Eosin Blue	100	65	3	120	100	72.49
Fuchsin Acid	200	25	8	240	50	89.05

Eosin Blue and Fuchsin Acid dye solutions of 50, 100, 150, and 200 mg/L and 100, 200, 300, 400 mg/L respectively, and their suffered under different temperatures of 25, 35, 45 and 55 ºC in equilibrium time used to each dye, after fixing the other parameters under the optimal conditions.

Adsorption isotherm models

To assess the equilibrium adsorption characteristics of the examined dyes, two prevalent isotherm models, Langmuir and Freundlich, were utilized. The Langmuir model characterizes monolayer adsorption on a uniform surface with equivalent adsorption sites, while the Freundlich model depicts adsorption on heterogeneous surfaces with potential multilayer interactions.

The experimental data demonstrated that the adsorption of Eosin Blue onto the AC–ZnO–TiO_2 composite adhered to the Langmuir model, indicating monolayer adsorption on generally homogeneous active sites. Conversely, the adsorption of Fuchsin Acid was better represented by the Freundlich model, suggesting adsorption on a heterogeneous surface. The heterogeneity factor ($n > 1$) indicates that the adsorption process is advantageous.

Furthermore, Fuchsin Acid demonstrated a superior adsorption capacity (519.87 mg/g) in contrast to Eosin Blue (164.64 mg/g), potentially due to variations in dye structure and the physicochemical characteristics of the modified adsorbent (Al-Ghouti and Al-Absi, 2020). This difference in adsorption capacity suggests that Fuchsin Acid may be more effective for applications requiring high dye removal efficiency, as illustrated in the Langmuir and Freundlich plots in Figures 13–16.

The adsorption capacities obtained in the present study demonstrate competitive performance compared with previously reported adsorbents used for dye removal from aqueous solutions. The maximum adsorption capacity of Eosin Blue (164.64 mg/g) onto the AC–ZnO–TiO_2 composite is comparable to several modified carbon-based adsorbents reported in recent studies. Masoudian *et al.* (2019) reported efficient dye removal using titanium oxide nanoparticles loaded onto activated carbon derived from watermelon rind, demonstrating strong adsorption performance due to the presence of active surface sites and improved pore structure.

Activated carbon modified with nanosized metal oxides has been shown to significantly enhance dye adsorption capacity because the incorporation of metal oxides increases the number of functional groups and improves electrostatic interactions between the adsorbent and dye molecules. In such systems, adsorption capacities of approximately 138–166 mg/g have been reported for several dyes using metal-oxide modified activated carbon materials.

Moreover, the adsorption capacity obtained for Fuchsin Acid (519.87 mg/g) in the present study exceeds that reported for many conventional activated carbon adsorbents. The enhanced adsorption efficiency results from the synergistic interaction between activated carbon and ZnO–TiO_2 nanoparticles, which increases surface reactivity, adsorption site density, and pollutant–surface interactions. Previous research has demonstrated that combining nanostructured metal oxides with carbon-based materials can significantly improve pollutant removal efficiency due to enhanced adsorption and catalytic properties.

Thermodynamic functions

The effect of temperature on the adsorption process is essential to understand the mechanism and to evaluate the thermodynamic parameters. The distribution constant (k) was calculated using the ratio of solute concentration in the solid phase to that in the liquid phase, and then it was employed to estimate the standard Gibbs free energy change according to the equation (Wolski *et al.,* 2023) as follows:

$$\Delta G^{o} = -RT \ln K$$

Negative values of ΔG^{o} indicate that the adsorption process is spontaneous, whereas positive values suggest non-spontaneity. The relationship among the thermodynamic functions is expressed by the Gibbs equation:

$$\Delta G^{o} = \Delta H^{o} - T\Delta S^{o}$$

Both ΔHº and ΔSº can be obtained graphically from the linear plot of lnK versus 1/T. A positive ΔHº value corresponds to an endothermic process, while ΔHº indicates exothermic adsorption (Metyouy *et al.,* 2024).

Similarly, a positive ΔSº implies increased randomness and higher affinity of adsorbate molecules towards the adsorbent surface, whereas a negative s reflects decreased affinity.

ΔGº values were calculated and appeared as the negative value of all concentrations that refer to spontaneous adsorption reactions except at 200 mg/L in 25 ºC, indicating non-spontaneous adsorption of Eosin Blue. Spontaneity increased with temperature, suggesting physical adsorption. Enthalpy was exothermic at 100 mg/L but endothermic at higher concentrations. All entropy values were positive, reflecting the high affinity of the dye for the surface.

The negative change in free energy (ΔGº) values recorded for the adsorption of Fuchsin Acid onto modified activated carbon confirms that the adsorption reaction is spontaneous and tends to result in physical adsorption. A positive value of ΔSº indicated strong molecules of dye bound to the adsorbent surface. ΔHº was generally an endothermic adsorption process, except at a concentration of 200 mg/L, which tended towards exothermic behavior. The calculated thermodynamic parameters are presented in Tables 3 and 4.

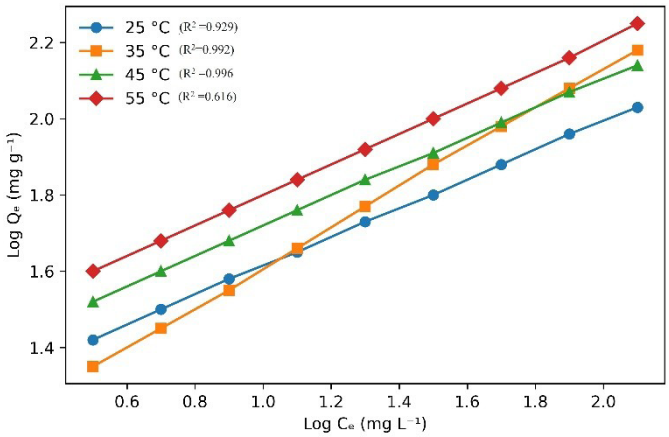

Figure 13. Freundlich adsorption isotherm model for Eosin Blue (EB) adsorption onto the AC–ZnO–TiO_2 composite

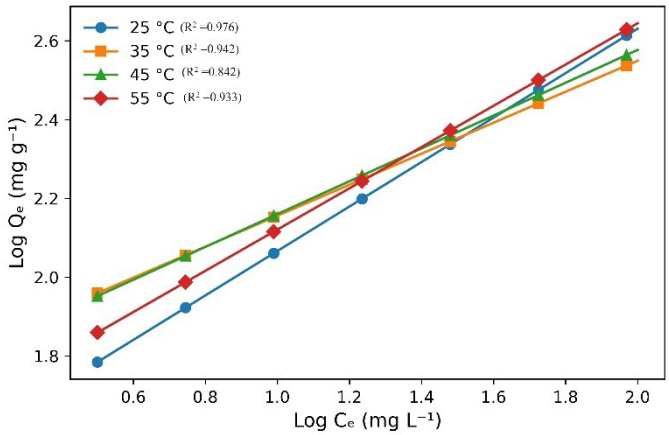

Figure 14. Freundlich adsorption isotherm model for Fuchsin Acid (FA) adsorption onto the AC–ZnO–TiO_2 composite

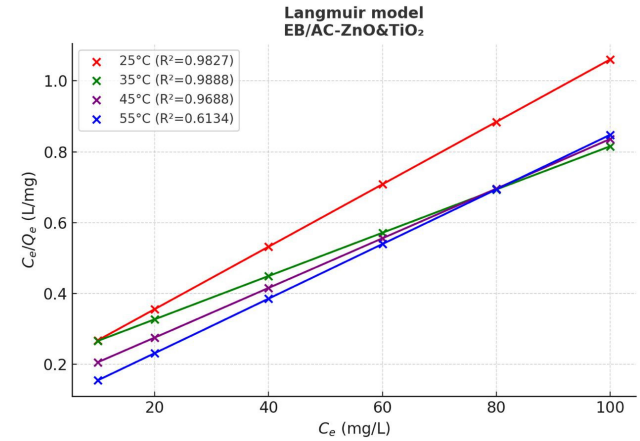

Figure 15. Langmuir adsorption isotherm model for Eosin Blue (EB) adsorption onto the AC–ZnO–TiO_2 composite

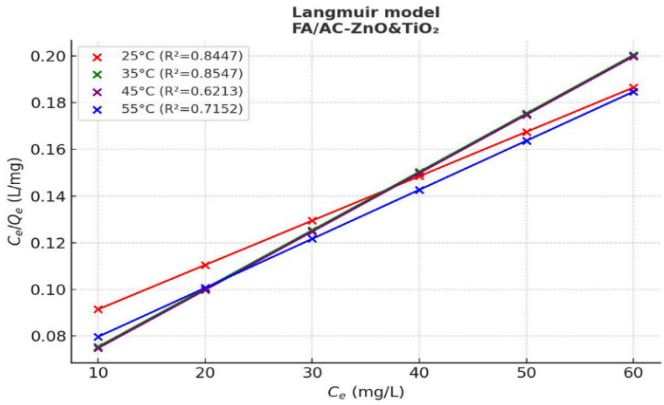

Figure 16. Langmuir adsorption isotherm model for Fuchsin Acid (FA) adsorption onto the AC–ZnO–TiO_2 composite

Table 3. Thermodynamic parameters for the adsorption of Eosin Blue onto the AC–ZnO–TiO_2 composite at different initial dye concentrations, including Gibbs free energy change (ΔG°), enthalpy change (ΔH°), and entropy change (ΔS°)

C_0 mg/L	ΔH° kJ/mol	ΔS° kJ/mol/K	ΔG° KJ/mol			
			298 °K	308 °K	318 °K	328 °K
50	29.949	0.110224	-3.1842	-3.5021	-5.1816	-6.3353
100	-2.00298	0.00136	-2.25447	-2.5212	-2.7491	-2.1890
150	15.9774	0.055565	-0.37406	-1.4862	-1.6539	-2.1430
200	38.12355	0.126699	0.108733	-0.9887	-1.0946	-4.1607

Table 4. Thermodynamic parameters for the adsorption of Fuchsin Acid onto the AC–ZnO–TiO_2 composite at different initial dye concentrations, including Gibbs free energy change (ΔG°), enthalpy change (ΔH°), and entropy change (ΔS°)

C_0 mg/L	ΔH° kJ/mol	ΔS° kJ/mol/K	ΔG° KJ/mol			
			298°K	308°K	318°K	328°K
100	-4.74964	0.004	-6.18328	-6.15017	-6.12725	-6.35688
200	-4.08991	0.003503	-5.12415	-5.18576	-5.20123	-5.23452
300	2.361965	0.018417	-3.11935	-3.32738	-3.48213	-3.68122
400	4.390698	0.026256	-3.43449	-3.6996	-3.94925	-4.227

4. Conclusion

The successful synthesis of activated carbon through oxidation, along with the preparation of zinc and titanium nano-oxide and their subsequent loading onto the activated carbon surface, resulted in a highly efficient adsorbent material. The prepared surface exhibited greater removal efficiency for Fuchsin Acid compared to Eosin Blue, demonstrating its high performance and selectivity. Thermodynamic analyses confirmed the spontaneity of the adsorption process, and the results revealed enhanced interactions between the adsorbent surface and dye molecules, involving both endothermic and exothermic contributions. These findings demonstrate the efficacy of the prepared surface for dye removal, making it a promising and sustainable option for wastewater treatment applications. The synthesized AC–ZnO–TiO_2 nanocomposite is suitable for the remediation of dye-polluted industrial wastewater, particularly from textile and dye production sectors. Moreover, subsequent research should concentrate on assessing the regeneration and reutilization capabilities of the adsorbent, as well as examining its adsorption efficacy in actual wastewater systems.

Acknowledgment

The authors sincerely thank the College of Science, Department of Ecology, in collaboration with the Marine Science Center, at the University of Basrah for their valuable support during this study.

Reference

Abdulnabi ZA, Al-doghachi FAJ, Abdulsahib HT. Synthesis, Characterization and Thermogravimetric Study of Some Metal Complexes of Selenazone Ligand Nanoparticles Analogue of Dithizone. Indones J Chem. 2021;21(5):1231-1243.

Abou-El-Souod GW, El-Sheekh MM. Biodegradation of basic Fuchsin Acidnd methyl red by the blue green algae Hydrocoleum oligotrichum and Oscillatoria limnetica. Environ Eng Manag J. 2016;15(2):279–86. Available from: http://omicron.ch.tuiasi.ro/EEMJ

Afroze S, Sen TK. A review on heavy metal ions and dye adsorption from water by agricultural solid waste adsorbents. Water Air Soil Pollut. 2018; 229:225. https://doi.org/10.1007/s11270-018-3910-3

Al-Ghouti MA, Al-Absi RS. Mechanistic understanding of the adsorption and thermodynamic aspects of cationic methylene blue dye onto cellulosic olive stones biomass from wastewater. Sci Rep. 2020;10(1):14957. https://doi.org/10.1038/s41598-020-72996-3

Al-Mosawi FH, Al-Abbawy DA, Abbas AF. Synthesis, analytical and uptake behavior of copper, cadmium and lead by new Schiff-base chelating resin. Res J Chem Environ. 2022;26(12):106–11. Available from: https://faculty.uobasrah.edu.iq/uploads/publications/1670567360.pdf

Alvez-Tovar B, Scalize PS, Angiolillo-Rodríguez G, Albuquerque A, Ebang MN, de Oliveira TF. Agro-industrial waste upcycling into activated carbons: A sustainable approach for dye removal and wastewater treatment. Sustainability. 2025;17(5):2036. https://doi.org/10.3390/su17052036

Alwi RS, Gopinathan R, Bhowal A, Garlapati C. Adsorption characteristics of activated carbon for the reclamation of eosin Y and indigo, carmine-colored effluents and a new isotherm model. Molecules. 2020;25(24):6014. https://doi.org/10.3390/molecules25246014

Aremu OH, Akintayo CO, Naidoo EB, Nelana SM, Ayanda OS. Synthesis and applications of nano-sized zinc oxide in wastewater treatment: a review. Int J Environ Sci Technol. 2021;18(10):3237–56. https://doi.org/10.1007/s13762-020-03069-1

Ayyalusamy S, Mishra S. Optimization of preparation conditions for activated carbons from polyethylene terephthalate using response surface methodology. Braz J Chem Eng. 2018;35(3):1105–16. https://doi.org/10.1590/0104-6632.20180353s20160724

Bahramifar N, Tavasoli M, Younesi H. Removal of eosin Y and Eosin Blue dyes from polluted water through biosorption using Saccharomyces cerevisiae: Isotherm, kinetic and thermodynamic studies. J Appl Res Water Wastewater. 2015;2(1):108–14.

Bellot-Gurlet L, Lahlil S, Paris C. An introduction and recent advances in the analytical study of early synthetic dyes and organic pigments in cultural heritage. Heritage. 2023;6(1):39–65. https://doi.org/10.3390/heritage6010003

Bhatnagar A, Hogland W, Marques M, Sillanpää M. An overview of the modification methods of activated carbon for its water treatment applications. Chem Eng J. 2013; 219:499–511. https://doi.org/10.1016/j.cej.2012.12.038

Derikvandi H, Nezamzadeh-Ejhieh A. Increased photocatalytic activity of NiO and ZnO in photodegradation of a model drug aqueous solution: effect of coupling, supporting, particles size and calcination temperature. J Hazard Mater. 2017; 321:629–38. https://doi.org/10.1016/j.jhazmat.2016.09.056

Djamel A, Kamarchou A, Ammar Z. Removal of organic pollutants from wastewater by activated carbon prepared from dates stones of southern Algeria. J Fundam Appl Sci. 2023;15(1). Available from: https://www.researchgate.net/publication/366774051

Fernández-Peña, L., Guzmán, E., Ortega, F., Bureau, L., Leaoforte, F., Velasco, D., Rubio, R., luengo, G. (2024) Physico-chemical study of polymer mixtures formed by a polycation and a zwitterionic copolymer in aqueous solution and upon adsorption onto negatively charged surfaces. arXiv:2401.15327 https://doi.org/10.1016/j.polymer.20

Jumaa AA, Abduljaleel SA, Alhello AAN, Abdulnabi ZA. Effectiveness of TiO_2 nanoparticles in removing heavy-metal contaminants from Basrah River water. Univ Thi-Qar J Sci. 2024;11(2):206–10. https://doi.org/10.32792/utq/utjsci/v11i2.1224

Khan I, Saeed K, Khan I. Nanoparticles: properties, applications and toxicities. Arab J Chem. 2017; 12:908–31. https://doi.org/10.1016/j.arabjc.2017.05.011

Krishnan S, Chatterjee S, Solanki A, Guha N, Singh MK, Gupta AK, Rai DK. Aminotetrazole-functionalized SiO_2-coated MgO nanoparticle composites for removal of acid fuchsin dye and detection of heavy metal ions. ACS Appl Nano Mater. 2020;3(1):123–34. https://doi.org/10.1021/acsanm.0c02351

Kumari P, Alam M, Siddiqi WA. Usage of nanoparticles as adsorbents for wastewater treatment: an emerging trend. Sustain Mater Technol. 2019; e00128. https://doi.org/10.1016/j.susmat.2019.e00128

Liu J, Liu Y, Peng J, Liu Z, Jiang Y, Meng M, Ni L. Preparation of high surface area oxidized activated carbon from peanut shell and application for the removal of organic pollutants and heavy metal ions. Water Air Soil Pollut. 2018;229(12):4021. https://doi.org/10.1007/s11270-018-4021-9

Masoudian N, Rajabi M, Ghaedi M. Titanium oxide nanoparticles loaded onto activated carbon prepared from bio-waste watermelon rind for the efficient ultrasonic-assisted adsorption of Congo red and phenol red dyes. Polyhedron. 2019; 173:105–14.

Mehta P, Chelike DK, Rathore RK. Adsorption-based approaches for exploring nanoparticle effectiveness in wastewater treatment. Chem Select. 2024;9(25):e202400959. https://doi.org/10.1002/slct.202400959

Metyouy K, Benkirane L, Sánchez ME, Cara-Jiménez J, Plakas KV, Chafik T. Valorization of agricultural olive waste as activated carbon adsorbent for remediation of water sources contaminated with pharmaceuticals. Sustain Chem Environ. 2024; 6:100110. https://doi.org/10.1016/j.scenv.2024.100110

Muttil N., Jagadeesan S., Chanda A., Duke M., and Singh SK. Production, types, and applications of activated carbon derived from waste tyres: an overview. Appl Sci. 2023;13(1):257. https://doi.org/10.3390/app13010257

Nageeb M. Adsorption technique for the removal of organic pollutants from water and wastewater. Org Pollut Monit Risk Treat. 2013;7(5):1–28.

Nayeri D, Mousavi SA. Dye removal from water and wastewater by nanosized metal oxides modified activated carbon: a review. J Environ Health Sci Eng. 2020. https://doi.org/10.1007/s40201-020-00566-w

Nguyen CH, Tran HN, Fu CC, Lu YT, Juang RS. Roles of adsorption and photocatalysis in removing organic pollutants from water by activated carbon-supported titania composites: kinetic aspects. J Taiwan Inst Chem Eng. 2020; 109:51–61. https://doi.org/10.1016/j.jtice.2020.02.01

Paul A, Malik M, Yadav M, Malhotra I, Gupta S. Water treatment using chemically activated charcoal. J Sci Technol. 2020;5(3):72–8.

Raheem MA, Abdulnabi ZA, Al-Shawi AA. Synthesis and characterization of multiwalled carbon nanotubes decorated by ZnO and Ag_2O for removing methyl green and erythrosin B dyes. Adv Chem Sci Eng. 2025;49(1):1–11. https://doi.org/10.18280/acsm.490111

Rahman H. Utilization of eosin dye as an ion pairing agent for determination of pharmaceuticals: a brief review. Int J Pharm Pharm Sci. 2017;9(12):1–9.

Remmani R, Makhloufi R, Miladi M, Fukuoka A, Ruiz Canales A, Núñez-Gómez D. Development of low-cost activated carbon towards an eco-efficient removal of organic pollutants from oily wastewater. Pol J Environ Stud. 2021;30(2):1–8. https://doi.org/10.15244/pjoes/123456

Rezania S, et al. Recent advances in the adsorption of pollutants using carbon-based and metal-oxide nanoparticles. Appl Sci. 2024;14(24):11492. https://doi.org/10.3390/app142411492

Salleh MAM, Mahmoud DK, Karim WAWA, Idris A. Cationic and anionic dye adsorption by agricultural solid wastes: a comprehensive review. Desalination. 2011;280(1–3):1–13. https://doi.org/10.1016/j.desal.2011.07.019

Seow ZLS, Wong ASW, Thavasi V, Jose R, Ramakrishna S, Ho GW. Controlled synthesis and application of ZnO nanoparticles, nanorods and nanospheres in dye-sensitized solar cells. Nanotechnology. 2008;20(4):045604. https://doi.org/10.1088/0957-4484/20/4/045604

Taher HZ, Azeez NM, Najim SA. Poly aromatic hydrocarbons accumulated on Pholcidea spider webs in Basra Province. IOP Conference Series: Earth and Environmental Science. 2023;1158(3):032006. https://doi.org/10.1088/1755-1315/1158/3/032006

Tolkou AK, Kyzas GZ. Advanced technologies of water and wastewater treatment. Environments. 2024;11(12):270. https://doi.org/10.3390/environments11120270

Tripathi M, Singh S, Pathak S, Kasaudhan J, Mishra A, Bala S, et al. Recent strategies for the remediation of textile dyes from wastewater: a systematic review. Toxics. 2023;11(11):940. https://doi.org/10.3390/toxics11110940

Wang Y., Liu S., Zhao J., Meng X., and Li Z. Recent advances of photocatalytic application in water treatment: a review. Nanomaterials. 2021;11(7):1804. https://doi.org/10.3390/nano11071804

Wolski R, Bazan-Wozniak A, Pietrzak R. Adsorption of methyl red and methylene blue on carbon Bioadsorbents obtained from biogas plant waste materials. Molecules. 2023;28(18):6712. https://doi.org/10.3390/molecules28186712

Yuliusman Y, Nasruddin N, Sanal A, Bernama A, Haris F, Ramadhan TI. Preparation of activated carbon from waste plastics polyethylene terephthalate as adsorbent in natural gas storage. IOP Conf Ser Mater Sci Eng. 2017; 176:012055. https://doi.org/10.1088/1757-899X/176/1/012055